LUT University

Wood plastic composites with improved electrical and thermal conductivity

Rajan Rathish, Näkki Jonne, Layek Rama, Rainosalo Egidija

This is a Final draft version of a publication

published by Springer Nature

in Wood Science and Technology

DOI: 10.1007/s00226-021-01275-9

Copyright of the original publication:

© The Author(s), under exclusive licence to Springer-Verlag GmbH Germany, part of Springer Nature 2021

Please cite the publication as follows:

Rajan, R., Näkki, J., Layek, R. et al. Wood plastic composites with improved electrical and thermal conductivity. Wood Sci Technol (2021). https://doi.org/10.1007/s00226-021-01275-9

This is a post-peer-review, pre-copyedit version of an article published in Wood Science and Technology. The final authenticated version is available online at: http://dx.doi.org/10.1007/s00226-021-01275-9

This is a parallel published version of an original publication. This version can differ from the original published article.

Wood Plastic Composites with Improved Electrical and Thermal Conductivity

Rathish Rajan[1,2], Jonne Näkki[1], Rama Layek[2,3], Egidija Rainosalo[1]

[1]Research and Development, Centria University of Applied Sciences, Talonpojankatu 2, Kokkola 67100, Finland
[2]Department of Materials Science, Tampere University of Technology, P.O. Box589, Tampere 33101, Finland
[3]Department of Separation Science, School of Engineering Science, LUT University, Mukkulankatu 19, 15210 Lahti, Finland

Correspondence to: Rathish Rajan rathish.rajan@centria.fi

Abstract

Graphene nanoplatelets (GNP) are used to produce wood plastic composites (WPC) with improved electrical and thermal conductivity. The polypropylene/wood/GNP hybrid composites are produced by melt compounding followed by hot pressing. The effect of GNP loadings (5, 10, and 15 wt.%) on electrical conductivity, thermal conductivity, tensile properties, and thermal degradation of hybrid WPC containing 20 wt.% of wood flour is studied. The effect of fast and slow cooling rates during hot pressing on the surface resistivity of hybrid WPC is evaluated. Scanning electron microscopy of the tensile fracture surface and polished cross-sections of hybrid WPC is analyzed. The hybrid WPC containing 20 wt.% wood flour and 15 wt.% of GNP (PP-W20-G15) is measured to show surface resistivity of 2.05E+06 Ω/sq and thermal conductivity of 0.61 W/m.K. There is a significant increase in electrical and thermal conductivity of PP-W20-G15 when compared to WPC containing 20 wt.% of wood flour (PP-W20). The wood flour helps with the distribution of GNP in PP-W20-G15 by which the surface resistivity is improved when compared to PP filled with 15 wt.% GNP. It was found that the surface resistivity of PP-W20-G15 was dependent on the cooling rate used during the hot pressing. There is a considerable decrease in tensile strength and an increase in the tensile modulus of hybrid WPCs compared to PP-W20 and neat polypropylene.

Introduction

The demand for electrically conductive composites is on the rise due to the growing need for antistatic materials for various applications including packaging and electronics that are susceptible to electrostatic damage or in electromagnetic shielding applications *(Choi et al. 2019, Yadav et al. 2019)*. Compared to conventional antistatic materials that are used currently, conductive polymer composites are cheap, lightweight, flexible, and easy to design and manufacture. Electrically conductive composites prepared from polymers other than intrinsically conducting polymers usually incorporate electrically conductive fillers to introduce the electrical functionality in the polymer. Commonly used electrically conductive fillers include carbon black *(Al-Saleh et al. 2013, Choi et al. 2019, Yang et al. 2015)*, carbon nanotubes *(Al-Saleh et al. 2013)*, carbon fibres *(Yang et al. 2015)*, and graphene *(Haznedar et al. 2013)*.

The electrical resistance of air-dried wood is higher than 10^{12} Ω and for insulating plastics, it is equal to or higher than 10^{11} Ω *(Fu and Yuan 2017)*. The electrostatic charge is generated on the surface of insulating material due to the piezoelectric effect caused by friction or mechanical effect. Due to high electrical resistance, electrostatic charges are prevented from escaping by allowing electrostatic charge build up on the surface. The electrostatic discharge (ESD) can occur through the high-intensity transfer of charge between two objects of different electrostatic potential when contacted *(Moultif et al. 2017)*. Antistatic agents when applied as a surface coating or as an internal additive with polymers can prevent the electrostatic charge accumulation by decreasing the bulk

volume or surface resistivity. The resistance of packaging materials according to ANSI/ESD S541 is tabulated in Table 1.

Table 1: Classification of packaging materials based on surface resistance

Material designation	**Surface resistance (Ω)**
Electric field shielding	$<10^3$
Conductive	$<10^4$
Dissipative/Anti-static	$\geq 10^4$ - $<10^{11}$
Insulative	$\geq 10^{11}$

Bio-composites play an essential role in various industries as an alternative to materials from fossil-fuel *(Alemdar and Sain 2008)*. Wood-plastic composites (WPC) are bio-composites produced from wood fiber and synthetic or bio-based plastics. Currently, WPC is used in building & construction, automotive, and household applications. The applications of WPC can be expanded to new industries by tailoring the properties of wood-plastic composites. As an example, incorporating electrical and thermal conductivity in WPC can open its application to products demanding these functional properties. Conductive (electrical and/or thermal) thermoplastic compounds are available in the market for producing products requiring anti-static properties, electromagnetic interference shielding (EMI shielding), and for those products used in thermal management in the electrical and electronic industry *(Biron 2018)*.

Hybridization of WPC with functional inorganic fillers and nanofillers are of interest since these fillers can impart special functionality to the WPC. Hybrid polymer composites are those with two or more reinforcing materials embedded in a matrix polymer. Most of the

literature studies related to hybrid composites indicate that the hybridization results in multifunctional polymer composites. It is also understood from the related literature that there is a synergic effect of reinforcing fillers, which may increase certain properties of the composites *(Lee et al. 2011, Papageorgiou et al. 2016, Pedrazzoli and Pegoretti 2013, Pedrazzoli et al. 2015, Thwe and Liao 2003)*.

Graphene has received a lot of interest in recent years due to its exceptional mechanical, thermal, and electrical properties. Graphene is a two-dimensional allotrope of carbon made up of a single layer of sp^2 hybridized carbon atoms *(Phiri et al. 2017)*. The structures with several layers of carbon atoms are called graphene nanoplatelets (GNPs) which are reported to be used as nanofillers to improve the various properties of polymer nanocomposite even at a low filler loading *(Tripathi et al. 2017)*. A major challenge of using graphene as filler in polymer composites remains the high price compared to alternatives like carbon black. According to a recent study *(Batista et al. 2019)*, the research-grade graphene powder is priced at 1-50 $/g and mass-produced graphene is available from as low as $20/kg to $800/kg. The specialty carbon black is sold for $50/kg and high conductive carbon black cost around $25/kg *(Mertens 2017)*. Considering that the desired property is reached at a much lower graphene loading compared to carbon black and the multi functionalities offered, graphene is a reasonable choice as filler for developing polymer composites. Several processing methods such as in-situ, solution casting, and melt mixing are used to prepare thermoplastic polymer-based nanocomposites*(Tripathi et al. 2017)*. Since melt mixing is a well-established processing technique in the plastic industry, a lot of research has been devoted to graphene-based

polymer nanocomposites *(Kalaitzidou et al. 2007, Kim and Macosko 2009, Zhang et al. 2010, Zhao et al. 2007, Zheng et al. 2004)*. Those studies indicate that the addition of graphene improves mechanical properties of the nanocomposites at a lower filler content. In terms of electrical conductivity, the percolation threshold is reached at a higher GNP loading for the composites prepared by the melt mixing method, when compared to in-situ and solution mixing methods *(Khanam et al. 2016)*. Hence, the electrical conductivity in graphene-based nanocomposites prepared by the melt mixing method is achieved by sacrificing mechanical properties up to a certain degree due to agglomeration of graphene above a loading of more than 10 wt.%.

Few studies have reported on the influence of GNP's on the properties of WPC. Most of those were focused on the influence of GNP's on mechanical and thermal properties. Sheshmani et al. *(2013)* studied the polypropylene/wood/GNP system and reported that the tensile and flexural properties of the hybrid composites increased at 0.8 wt% of GNP content. They also indicated that strength decreased due to agglomeration when the content of GNP's was increased to 3-5 wt%. In another study, polyvinylchloride/wood/GNP system was developed to be used as electromagnetic interference shielding material *(Karteri et al. 2017)*.

To the best of the authors knowledge, no studies have been published which addresses the electrical and thermal conductivities of polypropylene/wood flour/GNP hybrid composites produced through melt mixing method followed by compression moulding. The electrical and/or thermally conductive fillers used to introduce electrical or thermal

conductivities in WPC may favorably or adversely affect other important properties of the hybrid WPC. Thus, it is important to study the electrical/thermal conductivities and the mechanical properties of the hybrid WPC. The objective of this study is to prepare polypropylene-based anti-static wood plastic composites containing GNP's that can be utilized to produce ESD safe products such as ESD safe enclosures or containers and ESD safe WPC composite decking.

Experimental

Materials

The WPC masterbatch containing 50 wt.% wood flour and polypropylene (PP) was purchased from a WPC granulate manufacturer. The softwood flour consists of spruce and fir with a maximum size of 500 μm. The masterbatch contains 3 wt.% of additives including MAPP. The GNP masterbatch PP @ 30% heXo-G V20 was purchased from NanoXplore Inc, Canada. The GNP in the masterbatch is heXo-G V20 with an average thickness of 20 nm (40 layers) and a flake size of 50 μm. The heXo-G V20 is commercially sold for $20/kg. The PP used in the masterbatch is an impact copolymer 4220H from Pinnacle Polymers. The polypropylene in WPC and the PP used to dilute WPC masterbatch was Moplen EP240H, which is an impact-resistant copolymer produced by LyondellBasell.

Preparation of hybrid wood plastic composites

The hybrid WPC's were prepared by two-stage melt compounding in a co-rotating twin-screw extruder ZSK 18 MEGAlab from Coperion, Germany. The barrel length of the

extruder was 72 mm and the outer diameter of the screw was 18 mm (D_o/D_i = 1.55). The pre-mixed wood plastic composites containing 24 wt.% (WPC1), 30 wt.% (WPC2), and 40 wt.% (WPC3) were prepared by diluting WPC-MB (50 wt.% wood flour) with Moplen EP240H. In the second stage, WPC1 (83.5 wt%)/GNP-MB (16.5 wt.%), WPC2 (66.6 wt.%)/GNP-MB (33.4 wt.%), and WPC3 (50 wt.%)/GNP-MB (50 wt.%) were melt mixed to produce PP-W20-G5, PP-W20-G10, and PP-W20-G15, respectively. The pre-mix was fed from the main feeder and GNP-MB was fed from the side feeder. The compounding was done at a screw speed of 150 rpm and the total feed rate was 5 kg/h. The extruder temperature was set to 190^{o}C until the melting zone and then it was set to 200^{o}C in the discharge zone. The extrudate was cooled in water and finally pelletized and saved for further use. The designations and composition of hybrid wood plastic composites are listed in Table 2.

The WPC plates were made by hot pressing the hybrid WPC pellets. The pressing was done in a manual hydraulic hot press at a temperature of 220^{o}C for 3 minutes with a press load of 3.5 MPa. Initially, a pre-heating time of 15 minutes was given before the load was applied. The size of the plates was 200 mm x 200 mm with a thickness of 3.6 – 3.8 mm. These plates were later CNC machined to test specimens.

Table 2: Designations and composition of hybrid wood plastic composites

Composites	**PP (%)**	**Wood flour (%)**	**GNP (%)**
PP	100	0	0
PP-W20	80	20	0
PP-W20-G5	75	20	5
PP-W20-G10	70	20	10
PP-W20-G15	65	20	15

Characterization

The surface resistivity measurement was done according to ASTM D257 – 07: Standard Test Method for DC Resistance or Conductance of Insulating Materials. Surface resistivity was measured by applying a voltage potential across the surface of the insulator sample and measuring the resultant current (I) as shown in Figure 1.

The electrode system is a circular flat metal plate type concentric ring electrode Vermason H108C (upper electrode) and H116BC (lower electrode). The power supply was TRACOPOWER MHV12 – 0.5 K6000P, 500 volts. Voltmeter used was Fluke 45 Dual display multimeter and ammeter was Keithley model 6485 Picoammeter. The measurement was taken at 500 V and was done in a room maintained at a temperature of 21^{o}C ±2. The current reading from picoammeter was noted 60 s after the start of measurement. The surface resistivity measurement of all other samples was taken following the same procedure. Two plates each with 100 mm x 100 mm and thickness of 3.6 – 3.8 mm were measured for all the samples. Results are an average of four measurements taken from both surfaces of the two plates. The surface resistance of PP-W20-G15 prepared by slow and fast cooling was measured following the same procedure explained above except that the thickness of the test samples was 2 mm and test voltage was 100 V. The surface resistivity was calculated from equation (1).

$$\text{Surface resistivity } \rho_s = \frac{\pi\,(D1+D2)}{(D2-D1)} Rs \qquad \text{(Equation 1)}$$

whereas D1 is the outer diameter of the inner ring in cm; D2 inner diameter of the outer ring in cm; Rs is measured resistance in ohms.

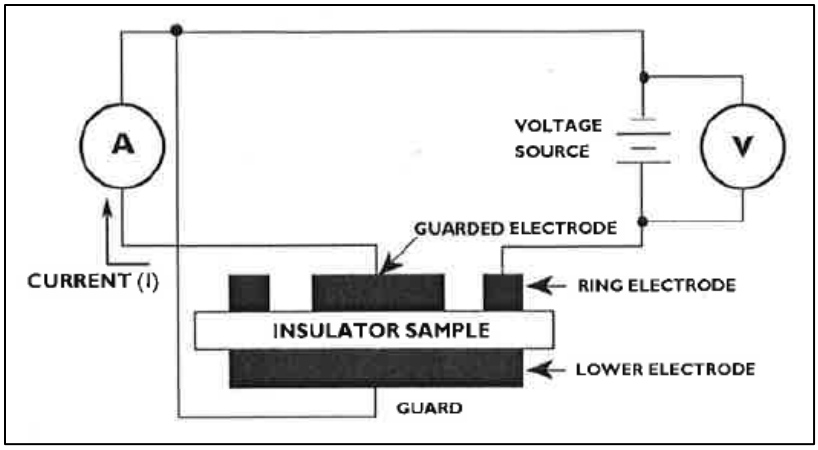

Figure 1: Surface resistivity measurement method

Netzsch LFA 467 device with Proteus LFA software was used to measure the thermal diffusivity and $C_P(T)$ of the samples at 25°C. Prior to the measurements, the surface of the sample was coated using a graphite spray. The rear surface of the samples was heated by exposing a short light xenon laser pulse on the rear surface and the temperature change of the opposite side of the sample was detected using an infrared detector. The thermal diffusivity was calculated using Equation (2) *(Parker et al. 1961)*.

$$\alpha = 0.1338\, d^2/t_{1/2} \qquad \text{(Equation 2)}$$

where α = the thermal diffusivity; d = thickness of the sample, and $t^{1/2}$ = time at the half signal height.

$$\kappa(T) = \alpha(T) \times c_P(T) \times \rho(T) \qquad \text{(Equation 3)}$$

The thermal conductivity of the samples was computed at 25°C using Equation (3). Where $\kappa(T)$, $\alpha(T)$, $c_P(T)$, and $\rho(T)$ are the thermal conductivity; thermal diffusivity; specific heat capacity, and experimental density of the sample respectively. The density of PP, PP-W20, PP-G15, and PP-W20-G15 was measured as 0.90, 0.94, 0.97, and 1.04,

respectively. The size of the specimens was 9.8 mm in diameter and 1.3 mm in thickness and the result presented is an average of 5 specimens.

The tensile test was performed according to ISO 527-2:2012 using a Tiratest 2705 tensile testing machine equipped with a 5kN load cell. The test was carried out at room temperature with a speed of 5 mm/minute. The length of the sample was 150 mm and the length of the narrow portion was 80 mm. The thickness of tensile specimens was 3.6 mm – 3.8 mm. Tensile properties are calculated as an average of 5 specimens. Tensile modulus is calculated from the slope of the stress/strain curve in the strain interval between 0.05% and 0.25%.

The examination of the platinum-coated tensile fracture surface was performed on JEOL JCM-6000 Neoscope scanning electron microscope with an electron acceleration voltage of 15 kV. For polished cross-section surfaces, the examination was made without a coating and with an acceleration voltage of 1 kV to reduce charging of the surface on Zeiss EVO 50VP scanning electron microscope.

Thermal degradation of the hybrid WPC was studied using a thermogravimetric analyzer, Netszch TG 209. The test was conducted in a nitrogen atmosphere by heating from 25^{o}C to 800^{o}C at 10^{o}C/minute. The sample mass for all the composites was 20 mg (±2). The results from one of the two specimens tested are reported. The effect of cooling rate on melting and crystallization behavior of the PP-W20-G15 was determined using Netzsch DSC 204 in a nitrogen atmosphere. The sample mass for all the composites was 10 mg

(±2) and the results from one of the two specimens tested are reported. The first heating was done from a temperature of 25°C to 220°C at a rate of 40°C/min followed by isothermal heating for 20 min representing the press time of the composites. The cooling was done at two different cooling rates of 2°C/min or 40°C/min. The second heating was performed at 40 °C/min.

A one-way analysis of variance (ANOVA) was performed on the collected data to determine the statistically significant differences ($p = < 0.05$) among the surface resistivity, thermal conductivity, and tensile properties of the composites. A paired t-test was performed on surface resistivity data to determine the statistical significance between the slow and fast cooling rate on the surface resistivity of composites containing 20 wt.% of wood fibre and 15 wt.% GNP (PP-W20-G15). The statistical analyses were performed using a free and open-source statistical analysis software JASP (Version 0.14.1).

Results and discussions

Surface resistivity

The surface resistivity of PP/GNP and functionalized WPC is listed in Table 3. The percolation threshold is reached at 15% by weight in the case of PP/GNP and hybrid composites. The surface resistivity of PP-G15 and PP-W20-G15 decreased several orders of magnitude to 10^8 Ω/sq and 10^6 Ω/sq, respectively. The results from surface resistivity measurements indicate that the surface resistivity decreased by the incorporation of 15 wt% GNP in both PP and WPC containing 20% by weight of wood filler.

The electrical conduction mechanism in the insulating polymer/conductive filler composites is described based on the percolation theory. The electrical conductivity in those composites is due to free electron movement through the conductive path formed by conductive fillers at a critical filler loading. At this critical filler loading, there is a sudden increase in electrical conductivity after which it gets saturated. This critical filler concentration is known to be the electrical percolation threshold concentration *(Tripathi et al. 2017)*.

The result from this study is in agreement with the findings in the literature related to PP/GNP composites. The percolation threshold for PP/GNP composites prepared through melt extrusion was found to be above 10 wt.% (4.4 vol%) *(Imran et al. 2018)* and 15 wt.% (6.7 vol%) *(Park et al. 2007)*. The percolation threshold for PP/GNP and hybrid composites in this study is reached at 15 wt.% (6.7 vol%). The size of the GNP is an important factor affecting the electrical conductivity of extrinsically conductive polymers. The percolation threshold in PP/GNP composites was reported to decrease with increasing in the flake size *(Jun et al. 2018)*. The percolation threshold for PP composites containing GNP with flake sizes of 150 μm and 2 μm is 2.99 vol% and >9.29 vol%, respectively as reported in the literature *(He et al. 2017)*. They also found that a lower thickness of layers improves electrical conductivity. The GNP used in this study has an average flake size of 50 μm and an average thickness of 20 nm. Since the percolation threshold for hybrid WPC was the same as for PP/GNP as found in the present study, it is assumed that using GNP with a larger flake size will initiate the formation of the conductive network at a low percolation threshold and the thinner GNP can facilitate fast

electronic movement between the layers resulting in improvement of electrical conductivity in hybrid WPC's.

Table 3: Effect of GNP on the surface resistivity of PP/GNP and wood plastic composites

Composites	**Surface resistivity (Ω/sq)**	**SD**
PP neat	1.19E+14	5.34E+12
PP-W20	1.08E+14	6.19E+12
PP-G5	1.05E+14	7.25E+12
PP-G10	1.00E+14	3.55E+12
PP-G15	8.83E+08	8.43E+08
PP-W20-G5	4.96E+14	6.67E+12
PP-W20-G10	4.48E+14	1.90E+13
PP-W20-G15	2.90E+06	2.05E+06

The WPC containing 20 wt.% of fibre and 15 wt.% GNP is more conductive than PP with the same loading (15 wt.%) of GNP alone (Figure 2). The total insulating components (PP and/or wood) in both PP-G15 and PP-W20-G15 are 85 wt%. The total amount of conductive filler in both PP/GNP and hybrid composite being the same, the decreased surface resistivity of hybrid composite is due to the good distribution of GNP in the presence of wood filler. The SEM images from the polished surface of PP neat and hybrid WPCs are seen in Figure 3 (d). It is evident that in the presence of wood fiber, the GNP was well distributed compared to the PP-G15 composite (Figure 3 c). Good distribution of GNP helped with forming a more effective conductive path in PP-W20-G15 hybrid composite.

In general, an uncoated insulator sample accumulates charge during the examination. SEM images from a cross-section of GNP-filled PP-G15 and PP-W20-G15 that were

acquired with 1 kV show brighter areas. This can be explained as the “reverse” charging characteristic, where the local field effect in a conductive composite enhances the relative secondary electron emission in the isolated conductive grains *(Chung et al. 1983)*. Similar observations in polymer/carbon nanofillers filled composites are reported elsewhere *(Syurik et al. 2013, Syurik et al. 2012)*. Due to this phenomenon, the conductive filler is seen brighter in a dark insulating matrix. Due to a low acceleration voltage of 1 kV, both the penetration depth of primacy electrons and the escape depth of secondary electrons (SE) are low, and only near-surface information is obtained.

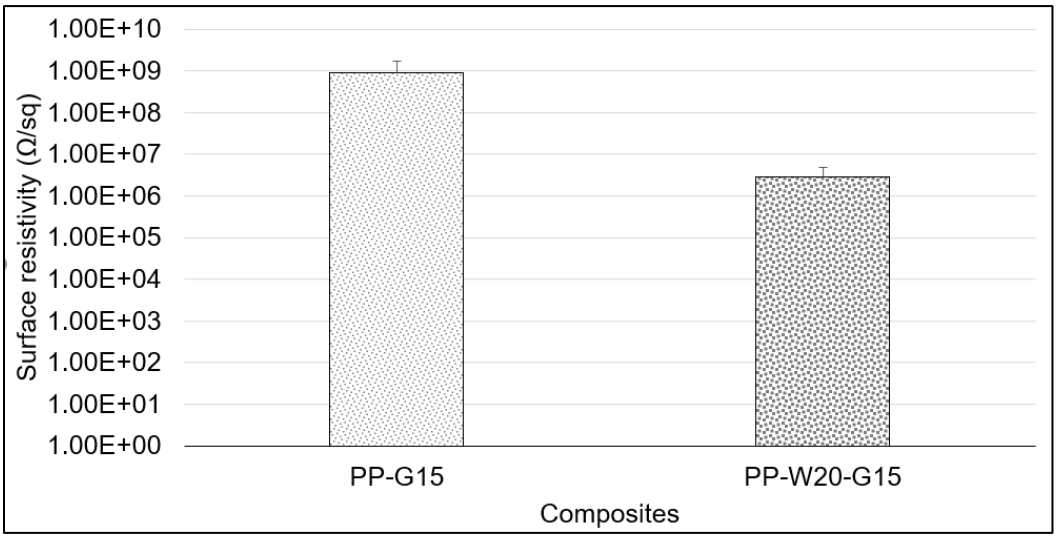

Figure 2: Surface resistivity of PP and wood plastic composites containing 15 wt.% of graphene nanoplatelets

The brighter GNP (15 wt%) is seen from Figure 3(c) and (d). In Figure 3(d), the GNP is seen to be even better distributed in the presence of 20 wt% wood fiber. The charging phenomenon directly represents the electrically conductive path of the GNP in the PP matrix as seen from the line marked in Figure 3(e) and (f). The results from SEM analysis support the findings from the surface resistivity measurements.

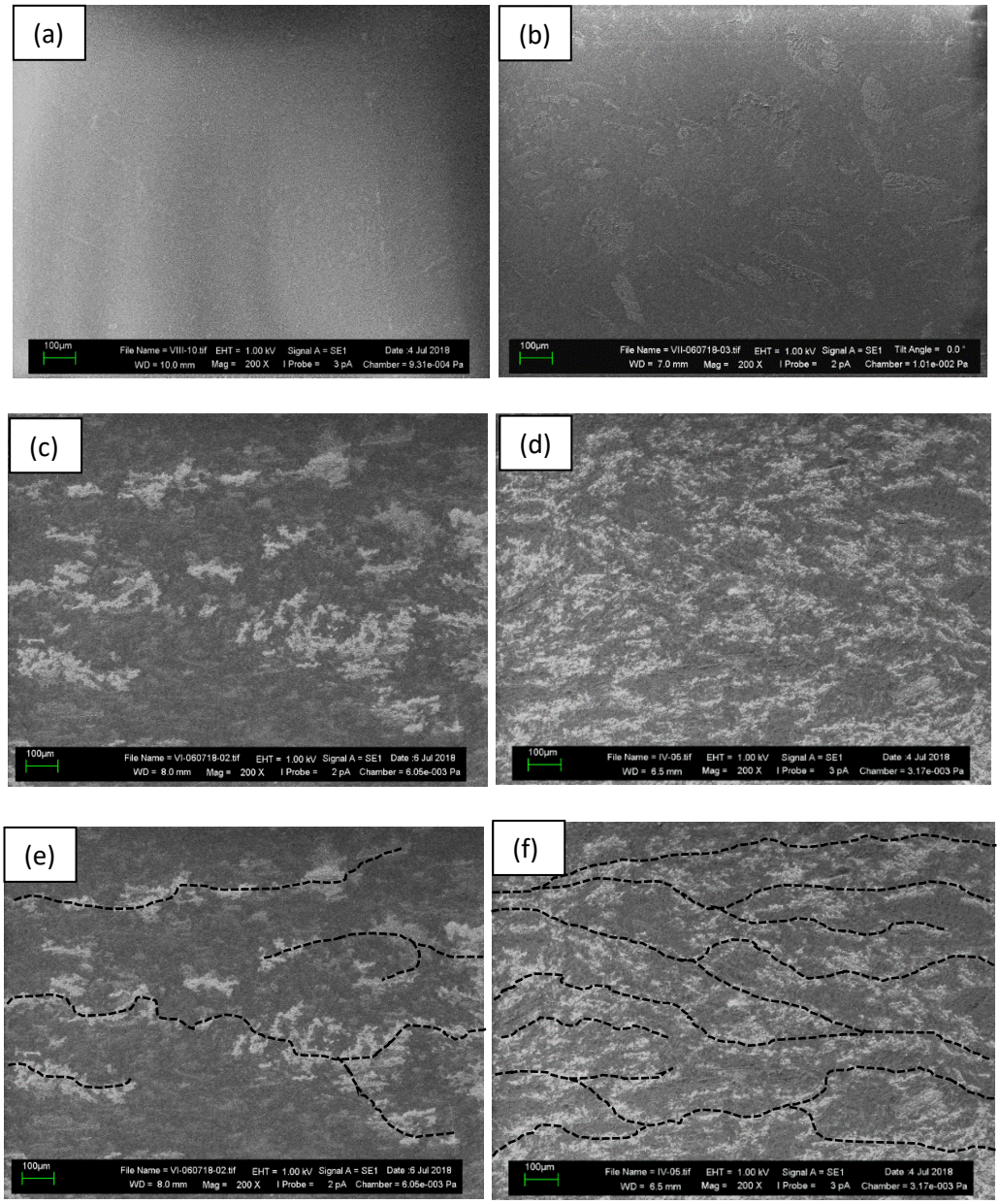

Figure 3: SEM images from the polished surface of (a) PP neat (b) wood plastic composite – PP-W20 (c) antistatic composites filled with GNP (PP-G15) (d) anti-static/dissipative wood plastic composite filled with wood flour and GNP (PP-W20-G15) (e) dotted lines representing the continuous conductive path of GNP in PP-G15 and (f) dotted lines representing continuous conductive path of GNP in PP-W20-G15

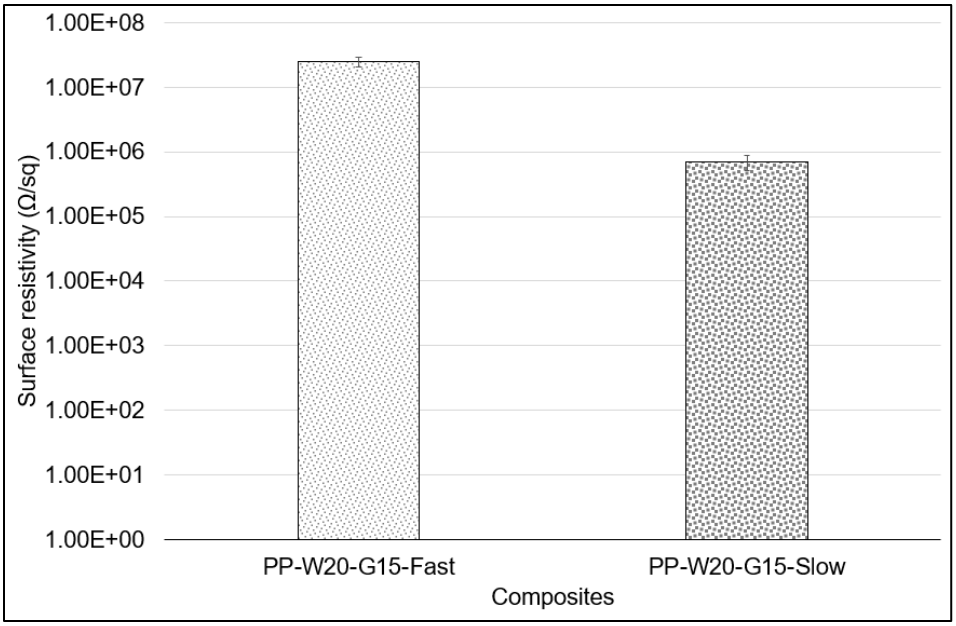

Figure 4: Effect of cooling rate of surface resistivity of hybrid wood plastic composites

The surface resistivity of PP-W20-G15 was found to be influenced by the processing conditions during the hot pressing (Figure 4). Two different cooling rates were used during the compression moulding; (1) fast cooling in which the composites were cooled at a rate of ≈14^{o}C/minute by running water and air through the channels in top and bottom platens in the hydraulic press and (2) slow cooling at a rate of ≈0.7^{o}C/minute, in which the composites were left in the press to cool down to 23^{o}C without using cooling water or air. The composite produced under slow cooling exhibits low surface resistivity (6.97E+05) compared to the composite produced under fast cooling (2.52E+07). Since there is no variation in GNP or wood flour content in the two composites, the lowering of resistivity can be related to the crystallization behavior of the polypropylene.

Table 4: Effect of cooling rate on the melting and crystallization behavior of composites

Composites	Tm (°C)		Tc (°C)		χ (%)	
	Fast	Slow	Fast	Slow	Fast	Slow
PP neat	169	170	106	128	30	34
PP-W20	172	169	104	129	29	34
PP-G15	175	174	106	131	30	37
PP-W20-G15	170	172	108	132	30	36

DSC analysis was done on the granulates of neat polymer and hybrid WPC to study the effect of fast and slow cooling on its thermal behavior. A cooling rate of 2°C/minute and 40°C/minute was used to represent slow cooling and fast cooling, respectively. It should be noted that the result presented in Table 4 does not represent the cooling rate used to produce composites. When comparing two different cooling rates, a notable difference in the case of crystallization temperature and the degree of crystallinity of PP can be observed from Table 4. The decrease in surface resistivity of PP-W20-G15-Slow produced using slow cooling can be correlated to the increase in the degree of crystallinity and crystallite size.

It is documented that the formation of the conductive path is easier in the case of highly crystalline thermoplastics compared to thermoplastics with a higher amorphous phase *(Chodak and Krupa 1999)*. According to Kalaitzidou et al. *(2008)*, not only the degree of crystallinity but also the type of crystals, size of the crystals, and nucleating effect of GNP can affect the percolation threshold and electrical resistivity of PP based composites. They found that the slow cooling resulted in the formation of larger, but fewer crystals compared to fast cooling in which a large number of small crystals were formed *(Kalaitzidou et al. 2008)*. A similar observation about decreased resistivity in the case of

slow cooled PP/CNT composites was made by Wang et al. *(2020)*. They reported that by using an external nucleating agent, most CNT was prevented from participating in the nucleation of PP crystals and therefore more CNT was available for forming a conductive path. Thus, the decreased resistivity of PP-W20-G15-Slow compared to PP-W20-G15-Fast is due to an increase in crystallinity and fewer, but large crystallites formed during slow cooling. It is assumed that the wood flour participated in the nucleation of PP crystals sparing most of the GNP to form a conductive path in the case of slow cooled PP-W20-G15 by decreasing the surface resistivity. Based on the results obtained from surface resistivity measurements and according to the literature *(Gulrez et al. 2014)*, the PP filled with 15 wt% of GNP and WPC containing 15 wt% GNP can be used in applications such as anti-static packaging for electronics and in wood plastic composites to prevent the static electricity build-up.

Thermal conductivity

The thermal conductivity of polypropylene (PP neat) and composites are shown in Figure 5. The incorporation of 15 wt.% GNP in wood plastic composites with 20 wt.% of wood filler has significantly increased thermal conductivity by 130% (PP-W20-G15). The increase in thermal conductivity is attributed to the better distribution of GNP in hybrid composites in the presence of wood flour as seen from Figure 5.

The GNP has high thermal conductivity and it is reported that incorporation of GNP in the polymer matrix can lead to an increase in thermal conductivity *(Li et al. 2017)*. The main factors affecting the heat conduction in polymer composites containing GNP are lateral

size and thickness, interfacial thermal resistance, dispersion of GNP, surface functionalization, and GNP concentration *(Li et al. 2017)*. The heat transfer in polymer composites containing low GNP in which the fillers are unable to connect each other is highly dependent on the interfacial interaction of graphene and polymer *(Li et al. 2017)*. Effective interaction between polymer and graphene can decrease the interfacial thermal resistance and improve the phonon transfer between polymer and graphene. In the case of polymer composites with higher GNP loading like those used in this study, the heat conduction is through the thermally conductive path formed by the GNP-GNP contact. Once the composite contacts with the heat source, the heat transfers quickly through the thermal conduction path formed by GNP. In the case of PP/GNP and PP/GNP/wood flour hybrid composites, there was no critical loading or percolation threshold identified. An increase in the thermal conductivity in both systems containing 15 wt% of GNP was observed.

A similar observation was made by other researchers in the case of hybrid WPC based on PE *(Zhang et al. 2019)*. The wood fibre content in this study was kept at a constant loading of 40 wt.% and the GNP content in this study was 3, 6, 9, and 12 wt.%. The thermal conductivity of the composite increased to ≈0.9 W/m.K at a GNP loading of 12 wt.%. The thermal conductivity of PP/GNP composite was reported to be improved by the addition of GNP *(Imran et al. 2018)*. The thermal conductivity increased from 0.2-0.25 W/m.K for PP to approximately above 0.8 W/m.K at a GNP loading of 16.7 wt.%. In this study, the introduction of 15 wt.% GNP has shown an increase in thermal conductivity of PP and WPC to 0.44 W/m.K and 0.61 W/m.K respectively. Although there was an

increase in thermal conductivity of PP and WPC after the addition of 15 wt% GNP, these materials are still not suitable for use in applications requiring heat dissipation.

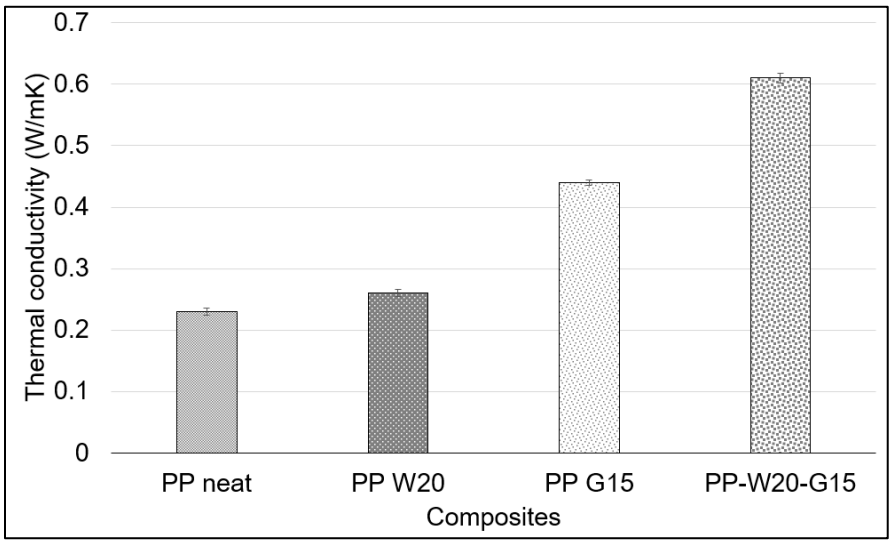

Figure 5: Effect of GNP loading on the thermal conductivity of wood plastic composites

Tensile properties

The tensile strength of PP-W20 and PP-Wood-GNP hybrid composites is shown in Figure 6. The strength of hybrid composites decreased gradually by increasing the GNP content. The strength of PP-W20-G10 and PP-W20-G15 decreased by 10% and 20% respectively when compared to PP-W20.

The capability of GNP in enhancing the tensile properties of composites is described based on graphene structure, dispersion of fillers, and filler-matrix adhesion *(Papageorgiou et al. 2017)*. The analysis of hybrid composites indicates that the composite's tensile strength is influenced by the presence of GNP fillers. The strength of PP-W20-G10 and PP-W20-G15 decreased (approx. 2 MPa and 4 MPa respectively)

when compared to the tensile strength (18 MPa) of PP-W20. However, because of the total filler content of PP-W20-G10 and PP-W20-G15 composites (30 wt% and 35 wt% respectively), the decrease in tensile strength is quite obvious. The WPC masterbatch used to produce PP-W20 and the hybrid WPCs contained 3 wt% of additives including MAPP. A widely accepted reaction mechanism of MAPP in WPCs proceeds with the reaction of maleic anhydride in MAPP with the free hydroxyl groups in wood flour to form an ester bond. The PP segment in the MAPP then becomes entangled with the melted neat PP resulting in a mechanical link between the hydrophilic wood flour and the hydrophobic PP *(Rowell 2006)*. However, there is an optimal concentration of MAPP until which the tensile strength increases. Excess addition of MAPP results in decreased tensile strength of composite *(Leu et al. 2012)*. Compared to neat PP, there was no significant decrease in tensile strength of PP-W20.

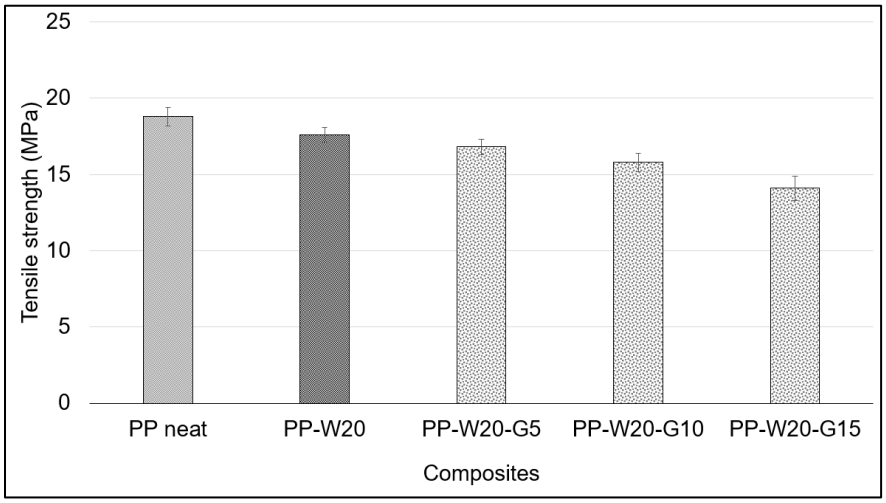

Figure 6: Effect of GNP loading on the tensile strength of hybrid WPC

Idumah and Hassan *(2016)* studied kenaf fibre/GNP/PP composite system and reported that usage of 5 wt% MAPP improved polymer to kenaf fibre adhesion. However, the adhesion of GNP to polymer was weak due to a lack of any chemical bond formation between GNP and MAPP. A similar observation is made from the tensile fracture surface analysis of the wood flour/GNP/PP composite system under this study. The nature of graphene to agglomerate has created stress concentration in the composite that leads to failure of composites in tensile load. The decrease in tensile properties due to the restacking of GNP at 5 wt% loading has been reported elsewhere *(Idumah and Hassan 2016)*. In this study, the GNP loadings in hybrid WPC are above 5 wt%. The decrease in tensile strength thus can be attributed to the agglomeration of the GNP and lack of chemical interaction between GNP and polymer.

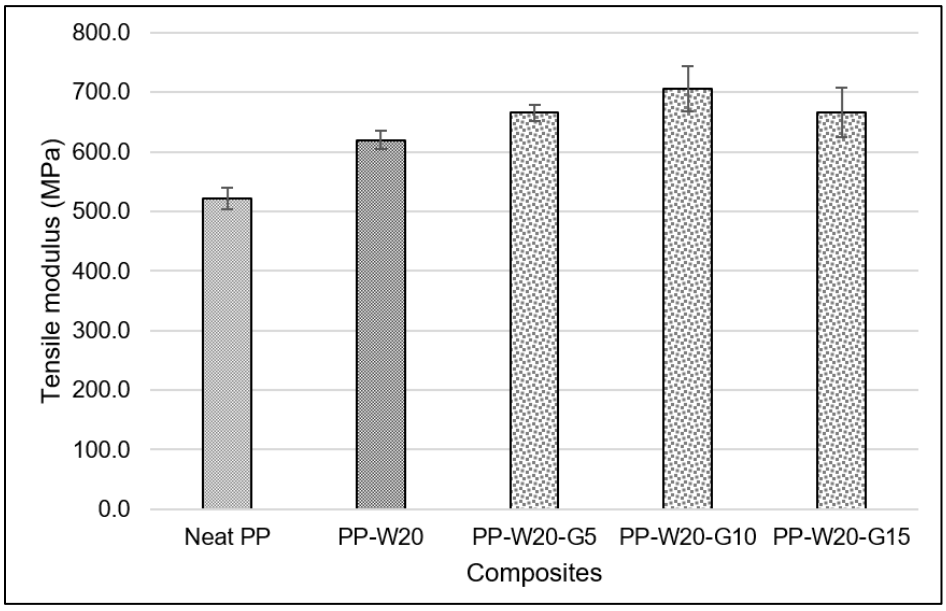

Figure 7: Effect of GNP content on tensile modulus of hybrid WPC

The Young's modulus of hybrid composites increased 35% when compared to PP neat and 14% compared to PP-W20 (Figure 7). The graphene is a two-dimensional layer of carbon that possesses high stiffness *(Potts et al. 2011)*. It seems that the reinforcing effect of graphene is increasing with increasing graphene content up to 10% by weight and then decreased. When compared to PP-W20, the elastic modulus of hybrid composite has improved. This indicates that the incorporation of GNP into wood plastic composite improved the stiffness of composites. The tensile modulus of graphene is 1 TPa *(de Sousa et al. 2015)*, and the increase in stiffness with the incorporation of GNP up to an optimal concentration of filler in nanocomposites and hybrid composites is also reported in the literature *(Kim et al. 2010, Sheshmani et al. 2013)*. The enhancement in the modulus can be attributed to the stiffness difference between the polymer and the graphene.

SEM images from the tensile fracture surface are shown in Figure 8 (a-d). The surface of wood flour in the wood plastic composite containing 20 wt% flour, seems to show good compatibility with PP (Figure 8a & b). The wood flour surface seems to be rough and wetted with the polymer. Further, there is less fibre pull out observed from the SEM analysis. These observations indicate good adhesion between PP and wood fibre in the presence of MAPP as a compatibilizing agent. The analysis of both PP-G15 and PP-W20-G15 revealed clusters of agglomerated particles appearing in different sizes. The surface of GNP was found to be clean without any polymer covering which indicates low compatibility between polymer and the GNP. From Figure 8(d), the partially pulled out and broken fibres seemed to be covered with polymer indicating better adhesion between

wood flour and PP in the hybrid composites. At the same time, the GNP surface is found to be without any polymer covering which indicates low compatibility with the PP in PP-W20-G15. The observations from SEM images support the finding from tensile testing which indicated the lack of adhesion between the polymer and GNP in the PP/wood/GNP system.

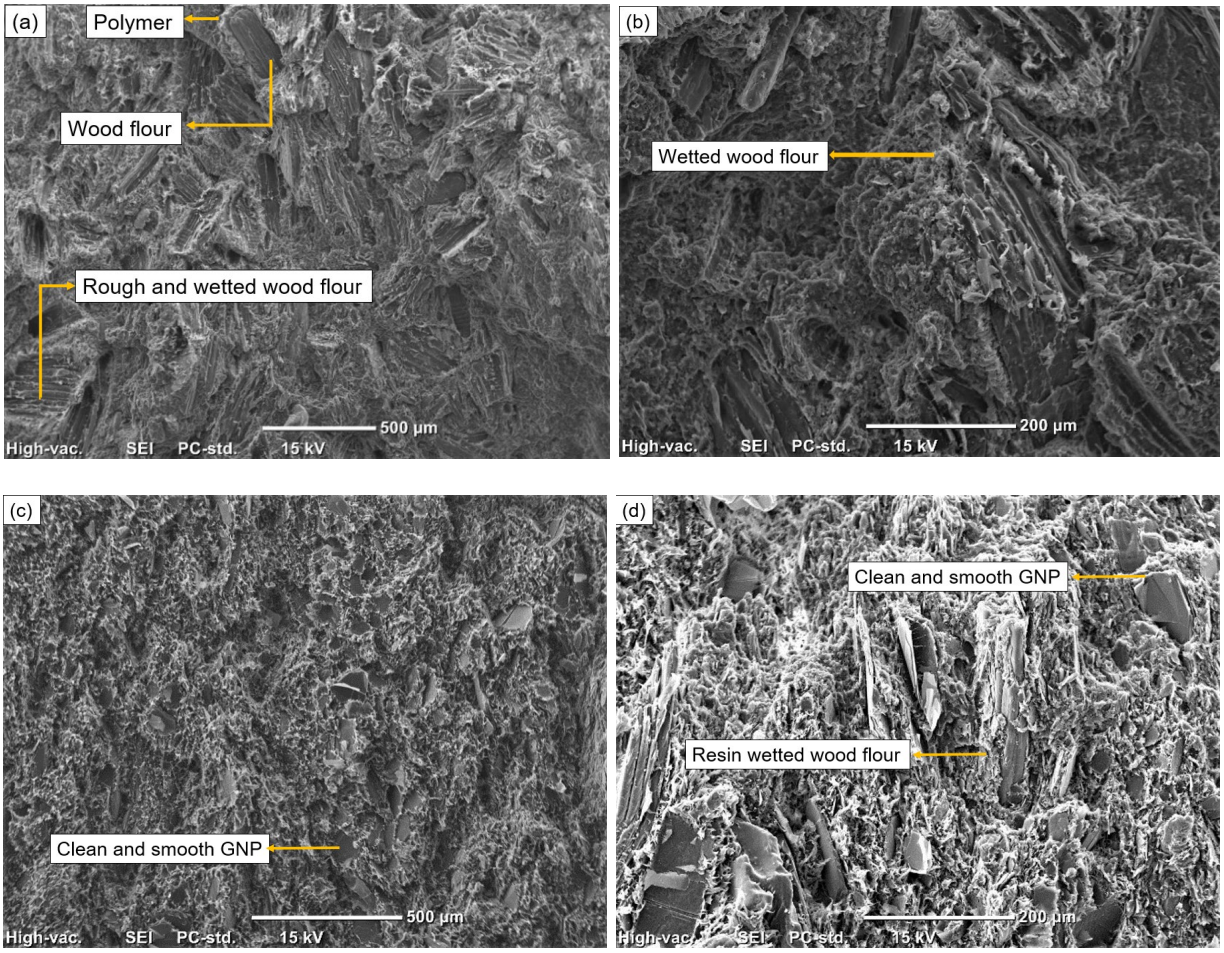

Figure 8: SEM images from the tensile fractured surface of PP-W20 (a), (b) and PP-W20-G15 (c), (d)

Thermogravimetric analysis

The TG and DTG curves from the thermogravimetric analysis are shown in Figure 9 and Figure 10, respectively. It is evident from the TGA analysis that the introduction of GNP increased the initial degradation temperature (2% mass loss) of PP by 78°C at a GNP loading of 15 wt% (PP-GNP). The initial degradation temperature of PP-W20 was determined to be 288°C and was found to be 52°C lower than PP neat. The PP neat and PP-G15 thermally decompose in a single stage. The increase in the initial degradation temperature of composites after the addition of GNP is reported in the literature *(Li et al. 2011)*. This is attributed to the barrier effect created through the tortuous path of GNPs formed in the matrix. The tortuous path can delay the diffusion of the condensed phase decomposition products to the surface or gas phase *(Liang et al. 2015)*. In addition, the absorption of free radicals produced during the decomposition by GNPs plays a key role in improving the thermal stability of PP-G15 *(Li et al. 2011, Liang et al. 2015)*.

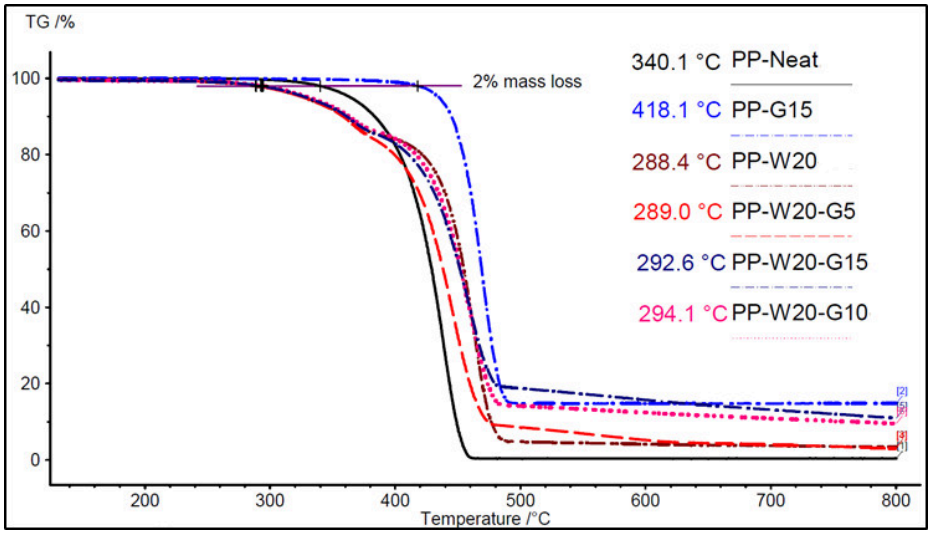

Figure 9: Thermograms of PP, PP/GNP, and hybrid wood plastic composites

The thermal decomposition of PP-W20 occurs in two stages as seen from Figure 10 (DTG). The first decomposition stage is mainly related to the degradation of wood flour in the composite and the second degradation stage mainly corresponds to the degradation of the polymer and remaining components of wood. In general, the wood fibre thermal decomposition occurs in three stages. (1) 250^{o}C - 340^{o}C is related to decomposition and depolymerization of hemicellulose and pectins; (2) 340^{o}C - 370^{o}C is ascribed to the decomposition of cellulose; (3) 370^{o}C - 500^{o}C is related to the decomposition of lignin *(Li et al. 2014)*. The first DTG peak (Figure 10) shows that the maximum degradation of wood flour in PP-W20 and all the three hybrid composites occurs between 360^{o}C – 380^{o}C.

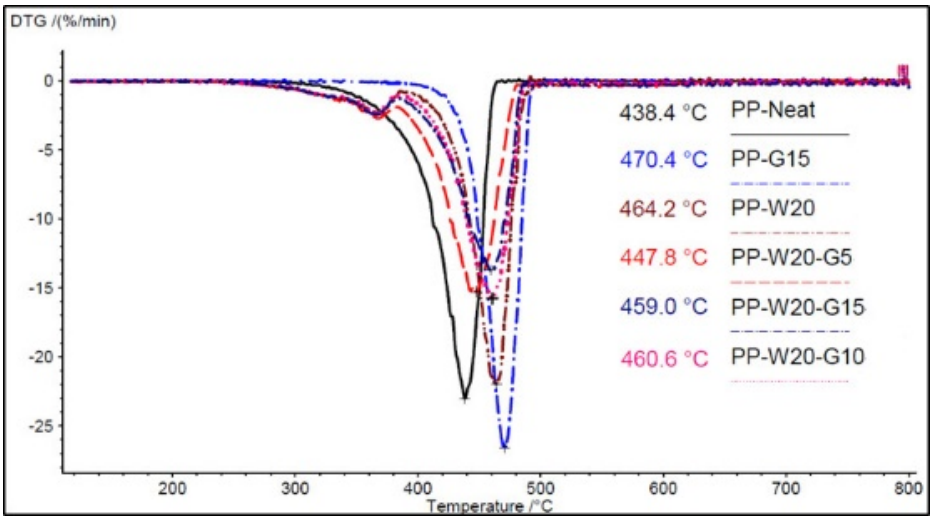

Figure 10: DTG curve of PP, PP/GNP, and hybrid wood plastic composites

The initial decomposition temperature (2% mass loss) of WPC increased slightly for PP-W20-G10 (294^{o}C) and PP-W20-G15 (293^{o}C) when compared to PP-W20 (288^{o}C). Although the improvement in thermal stability of hybrid composites is low compared to

PP-G15, the increase in initial thermal decomposition temperature of hybrid WPCs is due to the presence of GNP. As discussed earlier, GNP can delay the thermal decomposition by inhibiting the diffusion of oxygen and other volatiles formed during the decomposition of the hybrid WPCs.

The maximum degradation temperature (Tmax) of all the studied composites increased compared to PP neat (Figure 10). The increase in maximum degradation temperature of the composites compared to PP neat is due to the lignin content in wood flour and due to the increasing GNP content. The thermal stability of lignin is due to the presence of phenylpropanoid units consisting of highly stable aromatic phenyl groups *(Gordobil et al. 2015)*. The increase in Tmax for WPC compared to PP was reported elsewhere *(Sheshmani et al. 2013)*. They studied the thermal decomposition of the PP/WF/GNP system and reported an increase in initial decomposition temperature and Tmax after the addition of GNP. The maximum improvement in thermal stability was observed in the case of the hybrid composite containing 0.8 wt% GNP. Increasing the GNP content above 0.8 wt% decreased the thermal stability of hybrid composites. The maximum GNP loading used in their study was 5 wt% and in this study, it was 15 wt%. Thus, it is assumed that the higher content of GNP in hybrid WPCs lowered its effect on thermal stability due to the agglomeration of GNP.

Statistical analysis

The detailed results from statistical analysis are included as supporting information (See Electronic Supplementary Material). The test assumptions for one-way ANOVA on surface resistivity of composites were checked. Levene's test was significant ($p = < .001$),

indicating that the assumption of homogeneity of variance was violated. Normality was checked with a Q-Q plot and no deviations were noted. Since the assumption of homogeneity of variance was violated, Brown-Forsythe homogeneity correction was applied. According to ANOVA, there was a statistically significant difference among the composites on the surface resistivity ($p = <.001$). Games-Howell post-hoc test revealed that the surface resistivity results are statistically significant ($p = <.001$) except for PP-neat vs PP-W20 ($p = 0.225$), PP-G15 vs PP-W20-G15 ($p = 0.459$) and PP-W20-G5 vs PP-W20-G10 ($p = 0.079$). Although the post-hoc test shows no statistical difference between PP-G15 and PP-W20-G15, the experimental results indicate a difference between the two groups of composites. This is based on the findings from the cross-section SEM analysis of these two composites which supports the results from surface resistivity that PP-W20-G15 is more electrically conductive than PP-G15. The paired t-test was performed to differentiate the statistical significance between slow cooling and fast cooling of PP-W20-G15 on the surface resistivity. There was no deviation from normality as found from the (Shapiro-Wilk) test of normality. The t-test results show that there is a statistically significant difference in surface resistivity of fast cooled PP-W20-G15 and slow cooled PP-W20-G15 ($p = 0.001$).

As mentioned above, the test assumptions for ANOVA were checked and no deviations were noted in the case of thermal conductivity results. The ANOVA shows that there are statistically significant differences among the composites ($p = <.001$) in terms of thermal conductivity. Since there were no violations of assumptions, a Tukey post-hoc test was performed and the comparisons show that the thermal conductivity results have

statistically high significance (p = <.001 for all the comparisons except PP vs PP-W20 with p = 0.005). The comparison is considered as statistically significant when the p-value is <.05.

The ANOVA shows that there are statistically significant differences among the composites in terms of the tensile strength (p = < .001). Tukey's post-hoc comparisons show that compared to PP-neat, the tensile strength of all the hybrid WPC is statistically significant (p = <.001). When comparing to PP-W20, the tensile strength of PP-W20-G10 and PP-W20-G15 are statistically significant (p = 0.002 and p = <.001). There was no statistical significance between PP-W20-G5 and PP-W20-G10 (p = 0.139). Since the assumption of homogeneity of variances was violated, Brown-Forsythe homogeneity correction was applied in the case of tensile modulus of the composites. The ANOVA shows a statistically significant difference among the composites in terms of tensile modulus (p = < .001). Games-Howell post-hoc comparisons revealed that there is a statistically significant difference in hybrid WPC when compared to PP-W20. However, there was no statistically significant difference when comparing the hybrid WPC between each other.

Conclusion

The objective of this study was to develop wood plastic composites (WPC) with improved electrical and thermal conductivity. The graphene nanoplatelet used as conductive filler is found to be efficient in decreasing the surface resistivity of hybrid wood plastic composites. The percolation threshold for the studied composite is identified to be 15

wt.%. in the presence of 20 wt.% wood flour. The conductive path formation in the PP-W20-G15 composite is explained from the charge contrast in the SEM image taken at low voltage and high vacuum. The difference in the conductive path formation in PP-G15 and PP-W20-G15 is clear from the SEM images from the polished cross-section. The thermal conductivity shows an increasing trend with an increase in GNP loading. However, the increase in thermal conductivity from 0.23 to 0.61 W/m.K is of less significance when considering the practical applications like heat sink materials requiring a minimum thermal conductivity of 2.0 W/m.K. The decrease in the tensile strength of hybrid WPC is due to the weak interfacial adhesion between the PP and GNP. The adhesion between PP and wood in hybrid WPC was found to be good due to MAPP. This points out the need for using functionalized GNP while developing WPC containing WPCs. Improved interfacial adhesion can not only improve the mechanical properties but will also increase the thermal conductivity by decreasing the interfacial thermal resistance.

The antistatic wood plastic composite produced in this study can be utilized in producing ESD safe enclosures for sensitive electronic parts and in other applications demanding controlled electrostatic discharge. In the future, efforts should be focused on reaching the percolation threshold at lower GNP content considering the cost of GNP compared to conductive carbon black. In future, wood plastic composites containing conductive carbon black will be developed and studied as a cheaper alternative to graphene. Considering the moisture absorption ability of wood flour, a detailed study is required to see how the moisture absorption is affecting the various properties of electrically and thermally conductive wood plastic composites.

Acknowledgments

This study has received funding from EU Interreg IV North program 2014 - 2020 by The county Administrative Board of Norrbotten, Sweden and Regional Council of Lapland, Finland, for project SMART-WPC. The authors gratefully acknowledge the financial support received for the project. Authors are thankful to Ms. Zainab Al-Maqdasi, Luleå University of Technology for fracture surface SEM images and Mr. Juha Junkala, Centria UAS for assistance in laboratory.

References

Alemdar A, Sain M (2008) Biocomposites from wheat straw nanofibers: Morphology, thermal and mechanical properties. Composites Science and Technology 68:557-565. doi: 10.1016/j.compscitech.2007.05.044

Al-Saleh MH, Saadeh WH, Sundararaj U (2013) EMI shielding effectiveness of carbon based nanostructured polymeric materials: A comparative study. Carbon 60:146-156. doi: 10.1016/j.carbon.2013.04.008

Batista NL, Helal E, Kurusu RS, Moghimian N, David E, Demarquette NR, Hubert P (2019) Mass-produced graphene—HDPE nanocomposites: Thermal, rheological, electrical, and mechanical properties. Polym Eng Sci 59:675-682. doi: https://doi.org/10.1002/pen.24981

Biron M (2018) Chapter 7 - Plastics Solutions for Practical Problems. In: Biron M (ed) Thermoplastics and Thermoplastic Composites (Third Edition). William Andrew Publishing, pp 883-1038

Chodak I, Krupa I (1999) “Percolation effect” and mechanical behavior of carbon black filled polyethylene. J Mater Sci Lett 18:1457-1459. doi: 10.1023/A:1006665527806

Choi H, Kim MS, Ahn D, Yeo SY, Lee S (2019) Electrical percolation threshold of carbon black in a polymer matrix and its application to antistatic fibre. Scientific Reports 9:1-12. doi: 10.1038/s41598-019-42495-1

Chung KT, Reisner JH, Campbell ER (1983) Charging phenomena in the scanning electron microscopy of conductor-insulator composites: A tool for composite structural analysis. Journal of Applied Physics 54:6099-6112. doi: 10.1063/1.331946

de Sousa, Daniel Eurico Salvador, Scuracchio CH, de Oliveira Barra, Guilherme Mariz, Lucas AdA (2015) Chapter 7 - Expanded graphite as a multifunctional filler for polymer nanocomposites. In: Friedrich K, Breuer U (eds) Multifunctionality of Polymer Composites. William Andrew Publishing, Oxford, pp 245-261

Fu F, Yuan Q (2017) 12 - Electricity functional composite for building construction. In: Fan M, Fu F (eds) Advanced High Strength Natural Fibre Composites in Construction. Woodhead Publishing, pp 287-331

Gordobil O, Delucis R, Egüés I, Labidi J (2015) Kraft lignin as filler in PLA to improve ductility and thermal properties. Industrial Crops and Products 72:46-53. doi: 10.1016/j.indcrop.2015.01.055

Gulrez SKH, Mohsin MEA, Shaikh H, Anis A, Pulose AM, Yadav MK, Qua EHP, Al-Zahrani SM (2014) A review on electrically conductive polypropylene and polyethylene. Polymer Composites 35:900-914. doi: 10.1002/pc.22734

Haznedar G, Cravanzola S, Zanetti M, Scarano D, Zecchina A, Cesano F (2013) Graphite nanoplatelets and carbon nanotubes based polyethylene composites: Electrical conductivity and morphology. Materials Chemistry and Physics 143:47-52. doi: 10.1016/j.matchemphys.2013.08.008

He S, Zhang J, Xiao X, Hong X, Lai Y (2017) Investigation of the conductive network formation of polypropylene/graphene nanoplatelets composites for different platelet sizes. J Mater Sci 52:13103-13119. doi: 10.1007/s10853-017-1413-y

Idumah CI, Hassan A (2016) Characterization and preparation of conductive exfoliated graphene nanoplatelets kenaf fibre hybrid polypropylene composites. Synthetic Metals 212:91-104. doi: 10.1016/j.synthmet.2015.12.011

Imran KA, Lou J, Shivakumar KN (2018) Enhancement of electrical and thermal conductivity of polypropylene by graphene nanoplatelets. Journal of Applied Polymer Science 135:45833. doi: https://doi.org/10.1002/app.45833

Jun Y, Um JG, Jiang G, Yu A (2018) A study on the effects of graphene nano-platelets (GnPs) sheet sizes from a few to hundred microns on the thermal, mechanical, and electrical properties of polypropylene (PP)/GnPs composites. Express polymer letters 12:885-897. doi: 10.3144/expresspolymlett.2018.76

Kalaitzidou K, Fukushima H, Askeland P, Drzal LT (2008) The nucleating effect of exfoliated graphite nanoplatelets and their influence on the crystal structure and

electrical conductivity of polypropylene nanocomposites. J Mater Sci 43:2895-2907. doi: 10.1007/s10853-007-1876-3

Kalaitzidou K, Fukushima H, Drzal LT (2007) A new compounding method for exfoliated graphite–polypropylene nanocomposites with enhanced flexural properties and lower percolation threshold. Composites Science and Technology 67:2045-2051. doi: 10.1016/j.compscitech.2006.11.014

Karteri I, Altun M, Gunes M (2017) Electromagnetic interference shielding performance and electromagnetic properties of wood-plastic nanocomposite with graphene nanoplatelets. Journal of Materials Science: Materials in Electronics 28:6704-6711. doi: 10.1007/s10854-017-6364-1

Kim H, Abdala AA, Macosko CW (2010) Graphene/Polymer Nanocomposites. Macromolecules 43:6515-6530. doi: 10.1021/ma100572e

Kim H, Macosko CW (2009) Processing-property relationships of polycarbonate/graphene composites. Polymer 50:3797-3809. doi: 10.1016/j.polymer.2009.05.038

Lee S, Choi O, Lee W, Yi J, Kim B, Byun J, Yoon M, Fong H, Thostenson ET, Chou T (2011) Processing and characterization of multi-scale hybrid composites reinforced with nanoscale carbon reinforcements and carbon fibers. Composites Part A: Applied Science and Manufacturing 42:337-344. doi: //doi.org/10.1016/j.compositesa.2010.10.016

Leu S, Yang T, Lo S, Yang T (2012) Optimized material composition to improve the physical and mechanical properties of extruded wood–plastic composites (WPCs). Construction and Building Materials 29:120-127. doi: 10.1016/j.conbuildmat.2011.09.013

Li A, Zhang C, Zhang Y (2017) Thermal Conductivity of Graphene-Polymer Composites: Mechanisms, Properties, and Applications. Polymers 9. doi: 10.3390/polym9090437

Li A, Zhang C, Zhang Y, Li A, Zhang C, Zhang Y (2017) Thermal Conductivity of Graphene-Polymer Composites: Mechanisms, Properties, and Applications. Polymers 9:437. doi: 10.3390/polym9090437

Li X, Lei B, Lin Z, Huang L, Tan S, Cai X (2014) The utilization of bamboo charcoal enhances wood plastic composites with excellent mechanical and thermal properties. Materials & Design 53:419-424. doi: 10.1016/j.matdes.2013.07.028

Li Y, Zhu J, Wei S, Ryu J, Sun L, Guo Z (2011) Poly(propylene)/Graphene Nanoplatelet Nanocomposites: Melt Rheological Behavior and Thermal, Electrical, and Electronic Properties. Macromolecular Chemistry and Physics 212:1951-1959. doi: 10.1002/macp.201100263

Liang JZ, Wang JZ, Tsui GCP, Tang CY (2015) Thermal decomposition kinetics of polypropylene composites filled with graphene nanoplatelets. Polymer Testing 48:97-103. doi: 10.1016/j.polymertesting.2015.09.015

Mertens R (2017) NanoXplore plans a 10,000 ton graphene powder facility. In: https://www.graphene-info.com/nanoxplore-plans-10000-ton-graphene-powder-facility. Accessed Dec 31, 2020

Moultif N, Masmoudi M, Joubert E, Latry O (2017) 5 - Reliability and Qualification Tests for High-Power MOSFET Transistors. In: El Hami A, Delaux D, Grzeskowiak H (eds) Reliability of High-Power Mechatronic Systems 2. Elsevier, pp 155-197

Noorunnisa Khanam P, AlMaadeed MA, Ouederni M, Harkin-Jones E, Mayoral B, Hamilton A, Sun D (2016) Melt processing and properties of linear low density polyethylene-graphene nanoplatelet composites. Vacuum 130:63-71. doi: 10.1016/j.vacuum.2016.04.022

Papageorgiou DG, Kinloch IA, Young RJ (2017) Mechanical properties of graphene and graphene-based nanocomposites. Progress in Materials Science 90:75-127. doi: 10.1016/j.pmatsci.2017.07.004

Papageorgiou DG, Kinloch IA, Young RJ (2016) Hybrid multifunctional graphene/glass-fibre polypropylene composites. Composites Science and Technology 137:44-51. doi: //doi.org/10.1016/j.compscitech.2016.10.018

Park HM, Kalitzidou K, Fukushima H, Drzal LT (2007) Exfoliated graphite nanoplatelet (xGnP)/polypropylene
nanocomposites. SPE 7th Annual Automotive CompositesConference and Exhibition, ACCE 2007—Driving Performance and Productivity,

Parker WJ, Jenkins RJ, Butler CP, Abbott GL (1961) Flash Method of Determining Thermal Diffusivity, Heat Capacity, and Thermal Conductivity. Journal of Applied Physics 32:1679-1684. doi: 10.1063/1.1728417

Pedrazzoli D, Pegoretti A, Kalaitzidou K (2015) Synergistic effect of graphite nanoplatelets and glass fibers in polypropylene composites. Journal of Applied Polymer Science 132. doi: 10.1002/app.41682

Pedrazzoli D, Pegoretti A (2013) Silica nanoparticles as coupling agents for polypropylene/glass composites. Composites Science and Technology 76:77-83. doi: //doi.org/10.1016/j.compscitech.2012.12.016

Phiri J, Gane P, Maloney TC (2017) General overview of graphene: Production, properties and application in polymer composites. Materials Science and Engineering: B 215:9-28. doi: 10.1016/j.mseb.2016.10.004

Potts JR, Dreyer DR, Bielawski CW, Ruoff RS (2011) Graphene-based polymer nanocomposites. Polymer 52:5-25. doi: //doi.org/10.1016/j.polymer.2010.11.042

Rowell RM (2006) Advances and challenges of wood polymer composites. Proceedings of the 8th Pacific Rim Bio-Based Composites Symposium, Advances and Challenges in Biocomposites : 20-23 November 2006, Kuala Lumper, Malaysia. Kepong, Malaysia : Forest Research Institute Malaysia, c2006: ISBN: 9832181879: 9789832181873: pages 2-11.

Sheshmani S, Ashori A, Arab Fashapoyeh M (2013) Wood plastic composite using graphene nanoplatelets. International Journal of Biological Macromolecules 58:1-6. doi: 10.1016/j.ijbiomac.2013.03.047

Syurik J, Ageev OA, Cherednichenko DI, Konoplev BG, Alexeev A (2013) Non-linear conductivity dependence on temperature in graphene-based polymer nanocomposite. Carbon 63:317-323. doi: 10.1016/j.carbon.2013.06.084

Syurik YV, Ghislandi MG, Tkalya EE, Paterson G, McGrouther D, Ageev OA, Loos J (2012) Graphene Network Organisation in Conductive Polymer Composites. Macromolecular Chemistry and Physics 213:1251-1258. doi: 10.1002/macp.201200116

Thwe MM, Liao K (2003) Durability of bamboo-glass fiber reinforced polymer matrix hybrid composites. Composites Science and Technology 63:375-387. doi: 10.1016/S0266-3538(02)00225-7

Tripathi SN, Rao GSS, Mathur AB, Jasra R (2017) Polyolefin/graphene nanocomposites: a review. RSC Adv 7:23615-23632. doi: 10.1039/C6RA28392F

Wang J, Kazemi Y, Wang S, Hamidinejad M, Mahmud MB, Pötschke P, Park CB (2020) Enhancing the electrical conductivity of PP/CNT nanocomposites through crystal-induced volume exclusion effect with a slow cooling rate. Composites Part B: Engineering 183:107663. doi: 10.1016/j.compositesb.2019.107663

Yadav R, Tirumali M, Wang X, Naebe M, Kandasubramanian B (2019) Polymer composite for antistatic application in aerospace. Defence Technology. doi: 10.1016/j.dt.2019.04.008

Yang H, Gong J, Wen X, Xue J, Chen Q, Jiang Z, Tian N, Tang T (2015) Effect of carbon black on improving thermal stability, flame retardancy and electrical conductivity of polypropylene/carbon fiber composites. Composites Science and Technology 113:31-37. doi: https://doi.org/10.1016/j.compscitech.2015.03.013

Zhang H, Zheng W, Yan Q, Yang Y, Wang J, Lu Z, Ji G, Yu Z (2010) Electrically conductive polyethylene terephthalate/graphene nanocomposites prepared by melt compounding. Polymer 51:1191-1196. doi: 10.1016/j.polymer.2010.01.027

Zhang X, Zhang J, Wang R (2019) Thermal and Mechanical Behavior of Wood Plastic Composites by Addition of Graphene Nanoplatelets. Polymers 11:1365. doi: 10.3390/polym11081365

Zhao YF, Xiao M, Wang SJ, Ge XC, Meng YZ (2007) Preparation and properties of electrically conductive PPS/expanded graphite nanocomposites. Composites Science and Technology 67:2528-2534. doi: 10.1016/j.compscitech.2006.12.009

Zheng W, Lu X, Wong S (2004) Electrical and mechanical properties of expanded graphite-reinforced high-density polyethylene. Journal of Applied Polymer Science 91:2781-2788. doi: 10.1002/app.13460